# Evaluation of pressure and species concentration measurement using uncertainty propagation

*Georgios* Stefopoulos[*], *Stylianos* Rigas[†], *Panagiotis* Tsirikoglou[‡], and *Anestis I.* Kalfas[§]

AUTh, Department of Mechanical Engineering, Laboratory of Fluid Mechanics and Turbomachinery, 54124 Thessaloniki, Greece

**Abstract.** This paper presents a probabilistic uncertainty evaluation method as described in the Guide to the Expression of Uncertainty in Measurements (GUM) and its application to probe measurements on pressure and fuel concentration. All sources of unceratinties are expressed as probability distributions. Consequently, the overall standard uncertainty of the quantity can be calculated using the Gaussian error propagation formula. The result of the uncertainty evaluation yields the most probable value of the measurand and describes its distribution in terms of rectangular (standard uncertainty) or gaussian ("expanded" uncertainty) distribution. A pitot-static probe and a fuel-concentration stem probe are used in order to demonstrate the principle of the probabilistic uncertainty evaluation method. The uncertainty induced by the pressure and concentration data acquisition system as well as the calibration of the fuel-concentration probe are included in the analysis. The overall "expanded" uncertainties for the measured and calculated values are presented as a function of different inlet fuel flows. In addition to this, the individual sources of uncertainty to the overall standard uncertainty are presented and discussed. Moreover, the transformation of standard uncertainty to "expanded" uncertainty will provide the deviation of the measurement in a 95% or 99% normal distributed interval instead of a 67% rectangular distributed interval.

## 1 Introduction

The developments of last decades in the field of gas turbines have driven associated advances in the methods available for aerodynamic measurements. Pressure measurements are used in order to quantify aerodynamic aspects of the flow such as aerodynamic losses, pressure rise of a compressor etc. In addition to this, pressure measurements are also conducted in other fields of engineering such as biomedical engineering etc. One vast category of pressure measurements are the pressure probes which are the only practical way of measuring pressure distribution on a flow field of a gas turbine. A. Doukelis and K. Mathioudakis (2003) [1] presented a detailed account of a pneumatic measuring technique appropriate for flow field measurements in turbomachinery configurations, making use of long-nose 5-hole probes. Sources of error were also discussed, with particular attention on those that can be introduced by the nose geometry and the coordinate transformations. In another study, Gh. AlDoori and R. D. Buttsworth (2014) [2] investigated the mixing region generated downstream of an axisymmetric supersonic steam ejector nozzle using a pitot pressure probe. Pitot pressure measurements in supersonic wet steam jet flows were obtained and the analysis of measurements yielded the spreading rate of the free shear layers. G. Zaragoza and R. Goodall (2014) [3] described a test rig to measure properties for heat exchangers. For this reason, they performed thermal energy transfer and pressure drop across the exchanger measurements. Continuing, Q. S. Li et al (2012) [4] performed field measurements of wind effects on a building during typhoons. Investigation of wind characteristics and extreme suction pressures on the building was conducted using the abovementioned measurements. Pressure measurements are also used for biomedical applications in order to provide useful information. A. Garinei and R. Marsili (2014) [5] investigated the loads acting on the most critical components of a pump used for biomedical application.

As far as species concentration measurements are concerned they are used on a more wide scientific field such as automotive engineering, aerospace engineering, chemistry etc. S. Ch. McEnally and D. L. Pfefferle (1998) [6] performed species and soot concentration measurements in a methane/air nonpremixed flame and X. Mercier et al (2001) [7] measured the absolute concentration of minor species by cavity ring-down

---

[*] *Georgios* Stefopoulos: gtstefop@meng.auth.gr
[†] *Stylianos* Rigas: stylianosrigas@gmail.com
[‡] *Panagiotis* Tsirikoglou: ptsiriko@gmail.com
[§] *Anestis I.* Kalfas: akalfas@auth.gr

spectroscopy (CRDS) by analyzing the exponential decay of the CRDS signal.

According to the above, a realistic determination of the uncertainties of a measurement is essential for the further usage of the result. When reporting the result of a measurement of a physical quantity, it is obligatory that some quantitative indication of the quality of the result be given so that those who use it can assess its reliability. Without such an indication, measurement results cannot be compared, either among themselves or with reference values given in a specification or standard [8].

This paper applies the probabilistic uncertainty evaluation method described in the GUM guide [8] in order to quantify the uncertainty on measurements, application is on both a continuous variable (pressure measurements) and a discrete variable (species concentration measurement), which were used in order to quantify the mixing process in a test rig where the performance of novel fuel-air premixers is studied as presented by Stefopoulos et al (2014) [9].

## 2 Gum guide introduction

The most crucial part of this analysis is the detection of all sources of uncertainty that influence the result. In some cases the information appears on data sheets of the measuring instrument; in some cases such information is absent. For these cases information must be found and quantified. The procedure that must be followed in order to obtain the overall uncertainties is presented in the GUM method [8]. Behr et al (2006) [10] followed also the same procedure in order to evaluate the uncertainty with application to pressure probe measurements in turbomachines. According to this, a mathematical expression must be obtained between the measurand and the measuring physical quantity input (e.g. volts). The deviation $u(x_i)$ of each input quantity must be calculated, at this point the input must be categorized as a Type A or Type B random variable. Furthermore, if the input quantities correlate, covariance must be calculated. Finally, the calculation of the estimation of the measurand can be made and the combined standard uncertainty can be calculated, assuming it follows a rectangular distribution. The transformation of the standard uncertainty to "expanded" uncertainty will provide the deviation of the measurand but in a normal distribution and with a 95% level of confidence for k=2 or 99% level of confidence for k=3

## Nomenclature

| | |
|---|---|
| A | Area of fuel injection |
| A/F | Air to fuel ratio |
| BR | Blowing Ratio |
| [C] | Fuel concentration [ppm] |
| $C_{ref}$ | Fuel concentration at injection plane [ppm] |
| $e_r$ | Relative Error |
| k | Coverage factor |
| M | Molecular mass |
| $\dot{m}_f$ | Fuel mass flow |

| | |
|---|---|
| $\dot{m}_{air}$ | Air mass flow |
| $m'_f$ | Normalized concentration ($m_f/19.9\ 10^{-5}$) |
| $P_o$ | Total Pressure |
| $P_{st}$ | Static Pressure |
| $R_s$ | Variable resistance of combustible-gas sensor |
| $R_o$ | Calibration Resistance parameter |
| $u(x_i)$ | Standard uncertainty |
| $U(x_i)$ | "Expanded" uncertainty |
| $u_i(x_i)$ | Propagated uncertainty |
| $V_{out}$ | FCP output voltage |
| $v_x$ | Fuel axial velocity |
| $x_f$ | Fuel mole fraction |
| $y_f$ | Fuel mass fraction |

### Abbreviations

| | |
|---|---|
| DAQ | Data Acquisition |
| FS | Full Scale |
| FCP | Fuel Concentration Probe |
| GEP | Gaussian Error Propagation |
| GUM | Guide to the expression of uncertainty in measurements |

### Greek

| | |
|---|---|
| λ | air to fuel equivalence ratio |
| ρ | density [kg/m$^3$] |
| μ | Mean value |

### Subscripts

| | |
|---|---|
| f | Fuel ($C_4H_{10}$) |
| air | Air |
| i | Different measurand (input parameter) |
| ref | Reference |
| stoich | Stoichiometric |

## 3 Uncertainty evaluation method

The evaluation procedure can be structured in four logical steps proposed by Weise and Wöger [11]:

Step 1 - Development of a mathematical model based on the definition of the measurand that describes the measurement problem.

Step 2 - Gathering of uncertainty information (observations, data sheets, etc.) and converting them to probability distributions

Step 3 - Calculation of the result and the associated standard uncertainty by applying the model and propagating the uncertainties.

Step 4 - Presentation of the result and its "expanded" uncertainty.

Step 1 process is based on the physics of each different problem and in the results that the study needs to produce. In Step 2 all information about the input data has to be expressed by probability distributions. If the distributions of the measurement devices are known then they are used. If only the upper or lower limit of the uncertainty of the measurement device is known, a rectangular distribution is used. In Step 3 all the information collected in Step 2 are combined using the Gaussian error propagation formula. Finally, in Step 4 the presentation of the result can take place as "expanded" uncertainty which will have an increased level of confidence (95%) opposed to the standard uncertainty (67%).

Another major point of this procedure is the classification of the input data type. According to GUM, two different input data types can exist:

- Type A
  Statistical information gathered during the measurement (observed data)
- Type B
  Non-statistical information, which are known prior to the measurement (data sheets, etc.)

Having categorized the input data as Type A or Type B variables, the next step of the procedure, and the most crucial, is the detection of the sources of uncertainty. In fact, each measuring quantity on an experiment induces an uncertainty that diffuses into the results; therefore it should be found and quantified in order for the final result to have the correct uncertainty.

As mentioned before, if the upper and lower limit of uncertainty of a measuring device is known and the manufacturer cannot provide more information, a rectangular distribution is used. According to this, the calculation of a Type B variable will be as follows:

Assume we have a measuring device and the manufacturer specifies that the uncertainty of the measurand is ±a%. Assume also that this particular device measures a quantity (let it be Y) of x value. Thus, the uncertainty of the result for Y=x would be xa%=0,01xa and because the upper and lower margin are the same, the uncertainty of the final result would be Y=x ±0.01xa. From the above calculation one main problem arises. What is the frequency that the value of x would be on the positive or the negative interval, therefore a statistical analysis has to be conducted in order to quantify the frequency (probability) of x being on the positive or negative margin.

The above calculations will be done again but following this time the GUM method. Assuming a rectangular distribution of the uncertainty of the measurand (Fig. 1) we have:
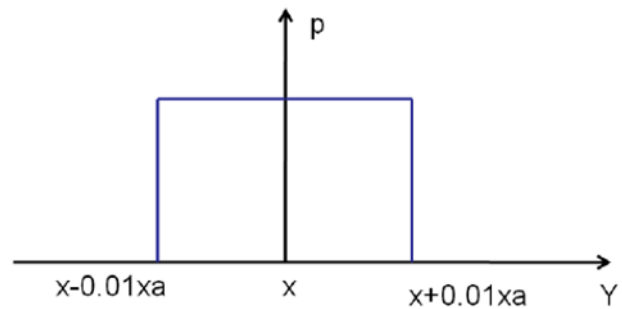


**Fig. 1.** Rectangular distribution of Y=x

The variance of this distribution is given by Eq. (1).

$$V(Y) = \frac{(2 \cdot 0.01xa)^2}{12} \tag{1}$$

And the standard deviation would be calculated as presented in Eq. (2).

$$u(Y) = \sqrt{V(Y)} = \frac{0.01\,x\,a}{\sqrt{3}} \tag{2}$$

The above result illustrates that if we measure Y=x and the measuring device has an uncertainty of ±a% then the uncertainty of the result would be Y=x $\pm \frac{0.01\,x\,a}{\sqrt{3}}$ which demonstrates a confidence interval with 67% level of confidence and following rectangular distribution.

Assume now that the measurand is not a function of only one input, but a more complicated function of different input data (e.g. Z=YK, where K is measured by another device with its respective upper and lower limit of uncertainty). In this case the Gaussian error propagation formula should be used in order for the overall standard deviation to be calculated and all uncertainties to be taken under consideration. Firstly, the uncertainty contribution of each input parameter on the result can be calculated using its partial derivative as shown in general at Eq. (3).

$$u_i(y) = \left| \frac{\partial y}{\partial x_i} \right| u(x_i) \, for \, i = 1,2,\dots,n \tag{3}$$

Continuing, using the Gaussian Error Propagation (GEP) formula the standard deviation (uncertainty) of the result which yields a 67% level of confidence can be calculated from Eq.(4).

$$u(y) = \sqrt{\sum_{i=1}^{n} u_i^2(y)} \, for \, i = 1,2,\dots,n \tag{4}$$

Finally, the GUM guide uses a term called "expanded" uncertainty which is calculated from Eq. (5).

$$U(y) = k \cdot u(y) \tag{5}$$

Where k is the coverage factor. For k=2 the uncertainty calculated by Eq. (4) is transformed to a normal distributed interval with a 95% level of confidence whereas for k=3 this interval has 99% level of confidence. For this work, the coverage factor was selected to have a value of k=2, thus all the presented "expanded" uncertainties are normally distributed and have a 95% level of confidence (Fig.2).
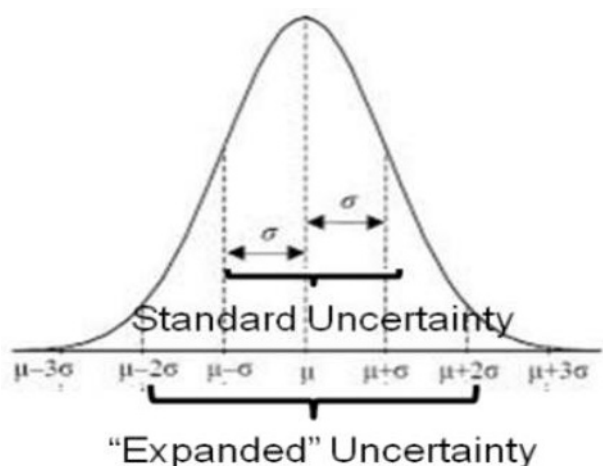
**Fig. 2.** Representation of "Expanded" Uncertainty versus standard Uncertainty.

# 4 Experimental method

The method of the uncertainty will be demonstrated on two different measurands, pressure measurements and fuel (isobutane, $C_4H_{10}$) concentration measurements. These measurements were conducted on a test rig where the aerodynamic mixing performance of novel fuel-air premixers is researched. In this investigation, a number of innovative fuel/air premixer designs have been developed and experimentally validated. Fuel passes through a tube in co-flow with air. The fuel delivery system involves a number of holes axially and circumferentially distributed along the tube. Consequently, fuel jets in cross-flow of air are generated and mixing with the co-flow of air occurs. Point measurements of pressure and fuel concentration were conducted in order to investigate the mixing process and entropy production (aerodynamic losses). All design variations have been investigated at four different injection fuel flows and the values of the blowing ratios are in the range of 0.24 to 1.00.

## 4.1 Pressure Data Acquisition System

As far as pressure measurements are concerned, a Pitot-Static probe was used in order to acquire radial measurements of total and static pressure. These measurements where used in order to quantify the aerodynamic losses each premixer induces in the flow. The DAQ of pressure was a 16-channel digital micro manometer. The datasheet of the manufacturer provided only the upper and lower limit of the uncertainty of the measurement which is ±0.05% of the measurand quantity. One point to be made is the fact that in order to measure the fuel mass flow injected into the premixer the pressure DAQ was used. According to this, the total pressure of the fuel on a large control volume and then its static pressure before the entrance-to-the-test-rig plane were measured and the calculation of fuel mass flow was feasible as it will be discussed in a later section.

## 4.2 Species Concentration Data Acquisition System

For the concentration data acquisition a 10-bit analog read of a microprocessor was used in order to read the exit voltage of a combustible gas sensor integrated on a probe (Fuel Concentration Probe- FCP). For this DAQ no information about the uncertainty of the measurand was available, so the uncertainty has to be found and quantified. The combustible gas sensor is supplied by 5 [V] DC. Depending on the fuel concentration it is exposed the resistance of the sensor changes, therefore the volt output changes according to the mathematical expression presented at Eq. (8).

$$[C] = \frac{Rs/Ro^{\frac{1}{0.612}}}{44776} \qquad (6)$$

Where Rs is the variable resistance of the sensor (which is a linear function of the output voltage and for the sake of brevity is not presented) and Ro a constant resistance that is calculated from the process of calibrating the FCP.

According to the above, the output voltage that the microprocessor reads is a dummy-continuous variable between 0 and 5 [V]. But due to the fact that the analog read is 10-bit, the microprocessor will map output voltages between 0 and 5 volts into integer values between 0 and 1023. This yields a resolution between readings of: 5 volts / 1024 units or, 0.0049 [V] (4.9 [mV]) per unit. According to this, an output voltage value of x [V] will be read as x only if it is at the form of x=s 0.0049, where s is an integer taking values from 0 to 1023. For instance, if the output voltage is x=2.45 then the actual value will be 2.45 since 2.45=500 0.0049 and a correct reading is occurred, but if the output voltage from the sensor is x=2.453 [V] then the reading value will be 2.4549, this is where the error of the analog read occurs. Judging from the above, the output voltage read from the microprocessor is a discrete variable and so its uncertainty will be.

# 5 Uncertainty of pressure measurements

As described in previous section the first process during the quantification of the uncertainty in measurements is the detection of the sources of uncertainty and the representation of the flow of uncertainty to the different calculated quantities. This is illustrated as a flow chart at Fig. (3) for quantities extracted via pressure measurements.
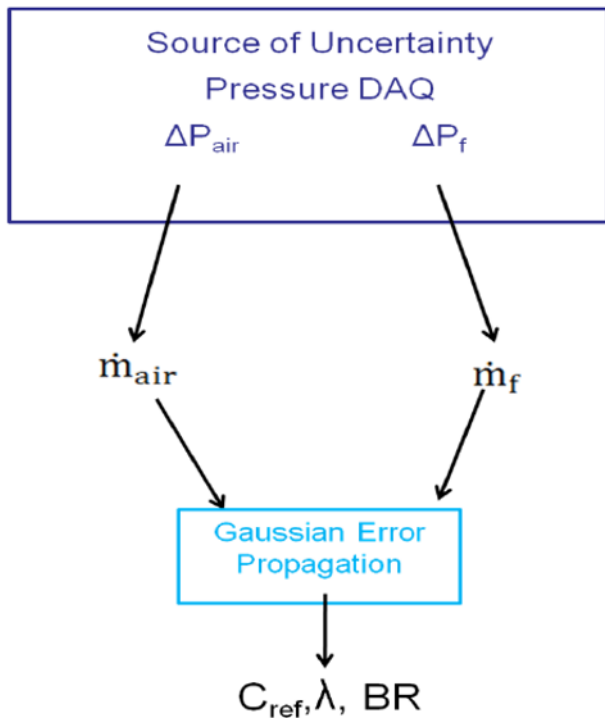
**Fig. 3.** Uncertainty propagation during pressure measurements

### 5.1 Step 1 – Development of the mathematical model

The calculation of $\dot{m}_f$ and $\dot{m}_{air}$ are feasible by conducting pressure measurements and subtracting them. For the first, the procedure followed is that explained in a previous section by measuring the total and static pressure of the fuel. Thus, using the known Bernulli equation presented at Eq. (7) the axial velocity $v_x$ of the fuel can be calculated and the calculation of its mass flow through the continuity equation (Eq. (8)) is feasible.

$$v_x = \sqrt{\frac{2(P_{o,f} - P_{st,f})}{\rho_f}} \qquad (7)$$

$$\dot{m}_f = \rho_f \cdot A \cdot v_x \qquad (8)$$

For the latter, the same equations are used and the total and static pressure are measured using a PitotStatic probe. During the process of the experiment the co-flow (air) mass flow was constant and in order to achieve the desired air to fuel equivalence ratios and BR the fuel mass flow was fluctuated. According to this, the uncertainty of the air mass flow is constant for different fuel mass flows whereas the uncertainty of fuel mass flow was variable.

The quantity $C_{ref}$ refers to the concentration (mole fraction) of fuel to the entrance plane. Since both $\dot{m}_{air}$ and $\dot{m}_f$ are known, using Eq. (9) one can calculate this variable.

$$x_f = \frac{\frac{y_f}{M_f}}{\sum \frac{y_i}{M_i}} = \frac{\frac{y_f}{58}}{\left(\frac{y_f}{58} + \frac{1 - y_f}{28.97}\right)} = C_{ref} \qquad (9)$$

Where $y_f$ is the mass fraction of the injected fuel and is calculated by Eq. (10)

$$y_f = \frac{m_f}{m_{air} + m_f} = \frac{\dot{m}_f}{\dot{m}_{air} + \dot{m}_f} \qquad (10)$$

Furthermore, the air to fuel equivalence ratio can be calculated using Eq. (11) and the BR parameter which is often used in bibliography (Karsten Kusterer et al (2008) [12], Muppidi (2006) [13]) to contradict the momentum of the fuel jets to the momentum of the co-flow can be calculated using Eq. (12).

$$\lambda = \frac{\left(\frac{A}{F}\right)}{\left(\frac{A}{F}\right)_{stoich}} = \frac{\left(\frac{\dot{m}_{air}}{\dot{m}_f}\right)}{\left(\frac{A}{F}\right)_{stoich}} \qquad (11)$$

Where $\left(\frac{A}{F}\right)_{stoich}$ is a parameter determined by the stoichiometry of the chemistry equation between clean air and isobutene and is constant with a value of 15.385.

$$BR = \frac{\rho_f v_f}{\rho_{air} v_{air}} \qquad (12)$$

### 5.2 Step 2 – Uncertainty Information

The manufacturer of the pressure DAQ provided only the upper and lower limit of uncertainty which is ±0.05% FS of the measurand quantity. Since no further information is available a rectangular distribution is assumed. The above value means that measuring for instance a pressure of 10 [Pa] an uncertainty of the result of 10 ± 0.005 [Pa] exists. However, for this particular investigation $P_o$ and $P_{st}$ was measured and the value that was being used was $\Delta P = P_o - P_{st}$. According to this, the GEP has to be used in order to find the uncertainty of $\Delta P$ which comes to be ± 0.0707% of the measurand as shown in Appendix A and again a rectangular distribution is assumed.

### 5.3 Step 3 – Uncertainty Calculation

During the process of the experiment the coflow (air) mass flow was held constant and in order to achieve the desired air to fuel equivalence ratios and BR the fuel mass flow was fluctuated. According to this, the uncertainties have been calculated for different fuel mass flows since the uncertainty of the co-flow (air) has a constant value for all experiment variations. To evaluate the contribution of each source of uncertainty on the overall uncertainty the GEP formula can be used.

### 5.4 Step 4 – Results

In order to understand the results it is vital to know the absolute (mean) values of the calculated quantities. Then, the "expanded" uncertainty of the result can be expressed as a margin and quantify the absolute uncertainty. Table 1 shows the different values of the calculated quantities.

**Table 1.** Air mass flow, Fuel mass flow/ Normalized fuel mass flow, Fuel concentration at inlet plane, air to fuel equivalence ratio, blowing ratio

| $\dot{m}_{air}$ [kg/sec] | $\dot{m}_f/\dot{m}'_f$ [kg/sec] | $C_{ref}$ | $\lambda$ | BR |
|---|---|---|---|---|
| 0.0252 | $19.9\ 10^{-5}$ /1 | $39.3\ 10^{-4}$ | 8.21 | 0.223 |
| | $44.5\ 10^{-5}$ /2.24 | $87.6\ 10^{-4}$ | 3.67 | 0.499 |
| | $62.9\ 10^{-5}$ /3.17 | $123.4\ 10^{-4}$ | 2.59 | 0.705 |
| | $89\ 10^{-5}$ /4.45 | $173\ 10^{-4}$ | 1.83 | 0.998 |

Increasing the injected fuel mass flow the blowing ratio (BR) of the fuel jets in co-flow is increased. Moreover, the fuel to air equivalence ratio decreases and the fuel concentration at the inlet plane increases. According to the above, the contribution of each input uncertainty $u_i(y)$ can be seen to the overall uncertainty. Fig. (4) presents the share of uncertainties for the various fuel injection mass flows for the parameters, BR and $\lambda$. The y-axis represents the square of the propagated uncertainty with the application of the GEP while the x-axis represents the various values of $\dot{m}_f$.
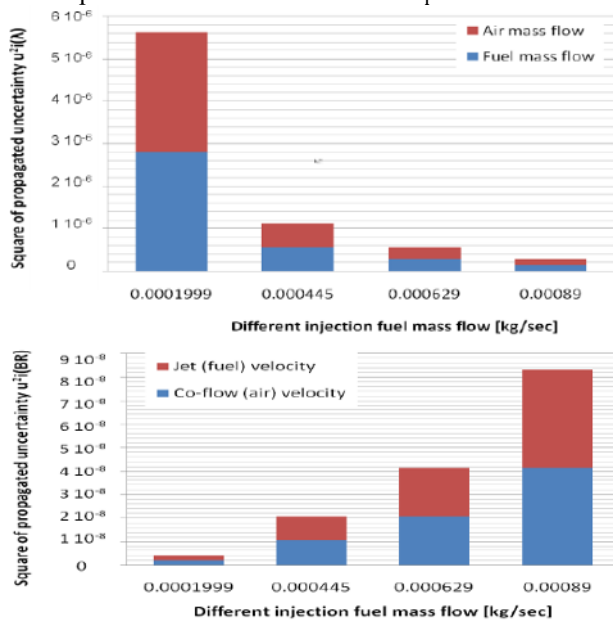


**Fig. 4.** Squares of propagated uncertainty $u_i^2(y)$ for $\lambda$ (top) and BR (bottom) and for four different fuel mass flows

Fig. (4) illustrates that the fuel mass flow strongly affects the uncertainty of the algebraic calculated values. The trend of those graphs is reversed. The uncertainty of $\lambda$ has a positive hyperbolic trend whereas the uncertainty of BR has an exponential trend. Furthermore, the contribution of each different source of uncertainty is the same (50%) for each different level of fuel mass flow for both parameters. The above can be explained by reviewing the mathematical expression of those two parameters (Eq. (11), Eq. (12)). According to this, both

parameters are defined as a fraction of $\dot{m}_f$ and $\dot{m}_{air}$ but in reverse. Another point to be made is the fact that the uncertainty of BR (Fig. (4) bottom) is two orders of magnitude lower than that of $\lambda$. This is due to the fact that a more complicated quantity is used to express $\lambda$ (mass flow) than BR (velocity), therefore the uncertainty rises. Moreover, in Fig. (5) the "expanded" (k=2) uncertainty of the above parameters is shown. The y-axis is logarithmic and represents the "expanded" uncertainty and the x-axis represents the various fuel mass flows.
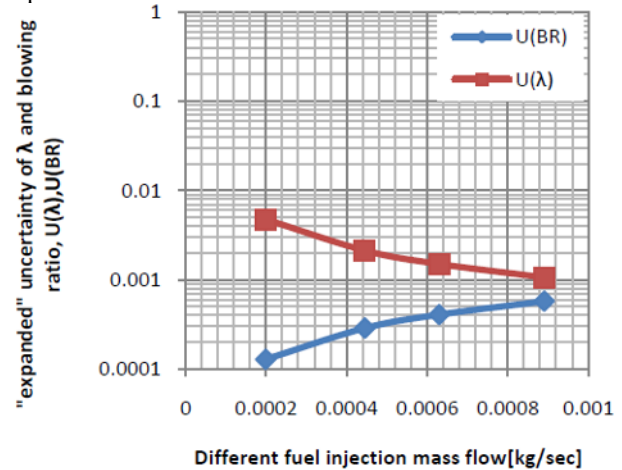


**Fig. 5.** Logarithmic representation for "Expanded" uncertainty $U(y)$ of air to fuel equivalence ratio (red) and blowing ratio (blue) for different fuel mass flows, k=2

The same behavior as presented before is present. The trend of the curves on a logarithmic plot tend to be linear, this means that we have exponential behavior. Furthermore, Fig. (5) demonstrates the deviation from the mean value. For instance, for $\dot{m}_f=0.000445$ the 95% normal distributed interval for $\lambda$ is ±0.00212 whereas for BR is ±0.00028. Comparing the deviation from the mean values presented at Table 1 the deviation is presented to be in acceptable margins and the relative error (Eq. (13)) is 0.1% for all the various fuel mass flows for both BR and $\lambda$.

The last two parameters defined from pressure measurements are $\dot{m}_f$ and $C_{ref}$. The "expanded" uncertainties of the above parameters are presented at Fig. (6)
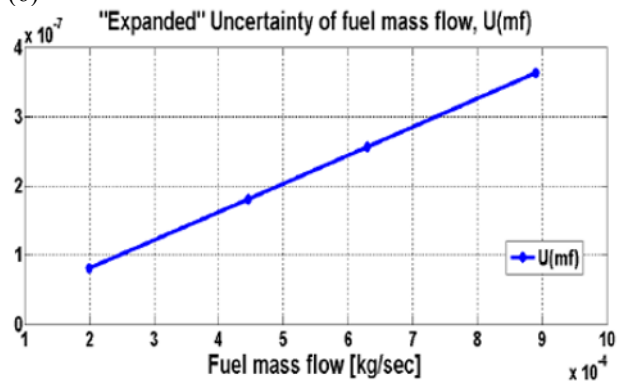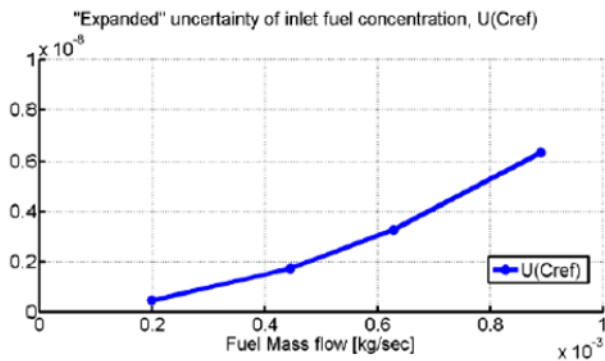
**Fig. 6.** "Expanded" uncertainty of fuel mass flow (top) and fuel concentration at inlet plane (bottom) for different fuel mass flows

As far as the uncertainty of fuel mass flow is concerned it is linear for the different levels of fuel mass flows. This is due to the fact that in order to calculate the uncertainty of $\dot{m}_f$, GEP was not used since there is only one uncertainty that is used for the calculation of the overall uncertainty (measuring the velocity of fuel injection). Moreover, by combining the initial uncertainties of fuel pressure measurements and air pressure measurements using the GEP and Eq. (8) & (9) the uncertainty of $C_{ref}$ can be calculated. This uncertainty has instead exponential trend since, as presented for BR and $\lambda$, it is a combination of both fuel and air pressure measurements. Again, the "expanded" uncertainty is actually a confidence interval. Thus, the deviation of $C_{ref}$ would be, for $\dot{m}_f$=44.5 $10^{-4}$, 87.6 $10^{-5}$ ±1.73 $10^{-9}$ whereas for $\dot{m}_f$ yields 44.5 $10^{-4}$ ±1.81 $10^{-7}$. Another point to be made is the fact that the uncertainty of $\dot{m}_f$ is three (3) orders of magnitude less than the mean value whereas the uncertainty of $C_{ref}$ is four (4) orders of magnitude less. This is due to the fact that a part of the uncertainty is actually "erased" during the calculation of mass fuel fraction through Eq. (9). The relative error for these parameters results in 0.08% for $\dot{m}_f$ and $10^{-5}$% for $C_{ref}$ and is constant for the various fuel mass flows.

# 6 Uncertainty of concentration measurements

In order to quantify the uncertainty induced from fuel concentration measurements a more complicated process is needed since the source of uncertainty is both from the measuring DAQ and from the calibration of the FCP as illustrated at Fig. (7).
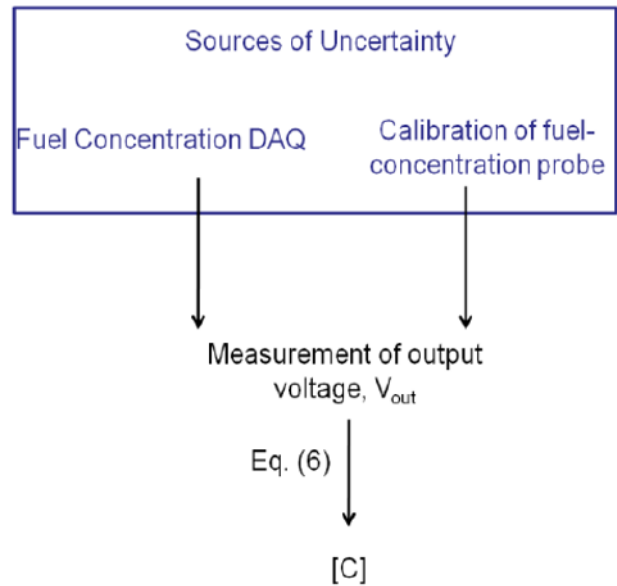


**Fig. 7.** Uncertainty propagation during fuel concentration measurements

## 6.1 Step 1 – Development of the mathematical model

The calculation of fuel concentration in [ppm] is feasible using the Eq. (6). As explained before the value if $R_s$ is a linear function of the output voltage which is the value read from the analogread. Thus, by reading the output voltage the concentration of fuel is known. The parameter of $R_o$ is a constant value and is defined from the calibration of the FCP on clean air where fuel concentration is zero.

## 6.2 Step 2 – Uncertainty Information

The "problem" that presented in a previous section of the analog read accuracy is used as uncertainty quantification for the concentration measurements. According to this, a rectangular distribution with margin of ±4.9 [mV] is assumed. This distribution is actually discrete. This means that the random variable (output voltage) will have a 33.3% chance of being on the positive margin and obtaining a value of $V_{out}$+4.9 [mV] and another 33.3% chance of being in the negative margin and obtaining a value of $V_{out}$-4.9 [mV] and a final 33.3% chance of a correct reading ($V_{out}$) to be occurred (Fig. (8)). The discrete standard deviation of the above can be calculated using statistics and yields $u(v_{out})$=4 $10^{-3}$ which is the uncertainty of the concentration DAQ. As far as the calibration of the FCP is concerned the same "problem" was present and affected the value of the parameter of Ro. In order of Ro to be defined the value of Rs was measured in clean air were [C]=0. The value obtained was normalized to the unknown yet value of Ro and the fraction, based on the manufacturer's datasheet, should yield a value of 5. According to this, the uncertainty of the initial measurement would be propagated to the calculation of the value of Ro which from a constant parameter (11472 [$\Omega$]) is transformed to a discrete

variable with an uncertainty (standard deviation) of ±0.7084.
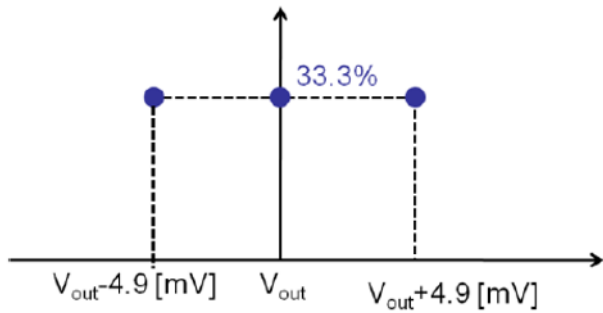


**Fig. 8.** Discrete rectangular distribution of $V_{out}$

## 6.3 Step 3 – Uncertainty Calculation

The uncertainty of the fuel concentration from calibration and measurement can be merged using the GEP and the total uncertainty during the measurement can be derived. Thus, the uncertainty of fuel concentration for different concentrations can be calculated. It is worth mentioning that the term "expanded" uncertainty cannot be defined here as the random variable is discrete and the normal distribution interval is undefined.

## 6.4 Step 4 – Results

The results from the propagation of uncertainty during fuel concentration measurements are presented at Fig. (9). The results show the discrete deviation of the measurement for a given value of concentration [ppm].
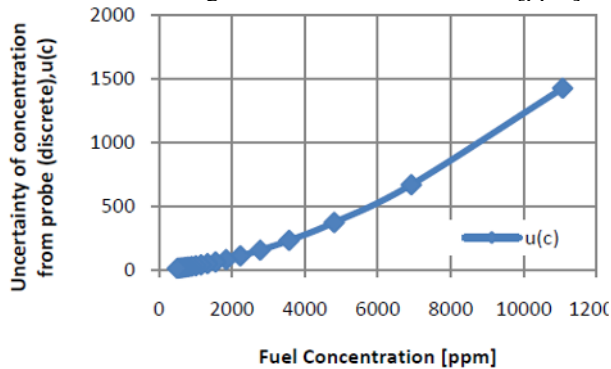


**Fig. 9.** Uncertainty (standard deviation, discrete) of fuel concentration measurements as a function of different concentrations [ppm].

Fig. (9) clearly demonstrates that the uncertainty during measurements with the FCP has an exponential trend. However, this uncertainty as discussed before is discrete. According to this, when measuring a value of [C]=4000 [ppm] this value has a standard deviation of ±350 [ppm]. Thus, the uncertainty of fuel concentration is only one order of magnitude less than the measuring quantity. For instance, if a measurement of 4000 [ppm] is occurred then there is 33.3% chance of it being approximately 3650[ppm] another 33.3% chance of it being 4350 [ppm] and finally a 33.3% chance of being 4000 [ppm]. Fig. (10) presents the relative error (Eq. (13)) of a concentration measurement using the FCP.
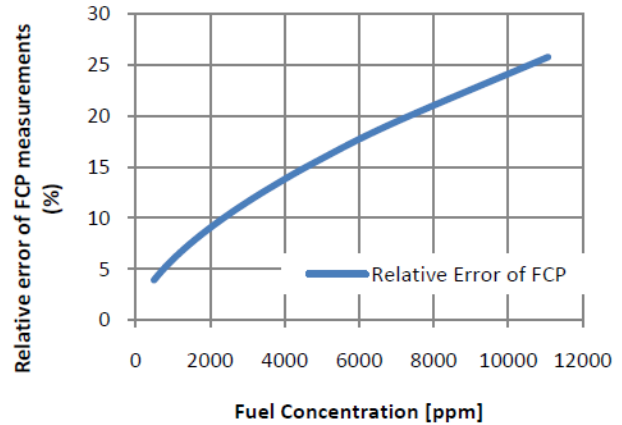
$$e_r = \frac{2 \cdot u(x)}{\mu} \qquad (13)$$



**Fig. 10.** Presentation of relative error ($e_r$) for different values of fuel concentration

The increment of relative error for concentration measurements is logarithmic. According to this, the usage of the FCP is prohibitive for measuring concentrations greater than 7.000 [ppm] since this is the critical value where $e_r$ is less than 20% of the measurement.

The contribution on the overall uncertainty of the calibration and the measurement of the FCP is illustrated at Fig. (11).
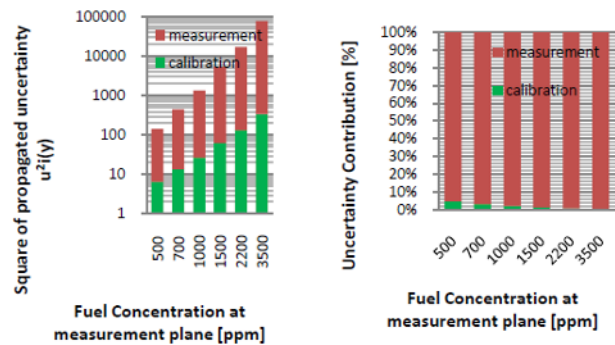


**Fig. 11.** Square of propagated uncertainties $u_i^2(y)$ on logarithmic axis (left) for 6 different fuel concentrations [ppm] and uncertainty contribution of calibration and measurement (right)

Fig. (11) demonstrates the square of propagated uncertainty on a logarithmic axis. Since on a logarithmic axis the contribution of calibration appears to be linear increasing this means that in general (as it can be seen by the graph on the right of Fig. (11)) they have a decreasing exponential trend. On the other hand, as we try to measure higher concentrations the uncertainty is mainly induced from the error of the analog-read and the calibration of the FCP does not have crucial role.

# 7 Uncertainty of combined measurements

The most complicated variable measured and calculated for the work mentioned before was the normalized fuel concentration at the plane of measurements. This variable ($[C]/C_{ref}$) is a normalization of the fuel concentration measured from the FCP ([C]) to the concentration at th entrance plane ($C_{ref}$). In order to calculate this variable and its uncertainty all the uncertainties must be merged together. The uncertainty of

the normalized concentration is in fact a fraction of a discrete variable and a continuous variable. Thus, the "expanded" uncertainty can be defined and is presented at Fig. (12) for different values of the normalized concentration and different inlet fuel injection mass flows.
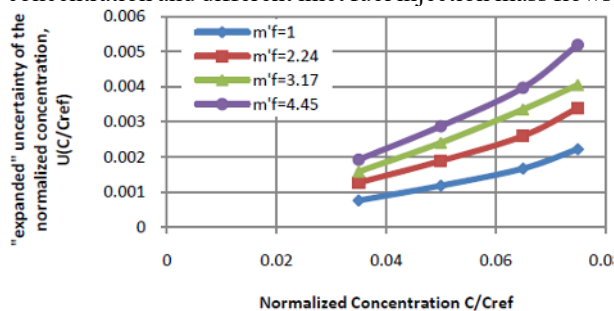


**Fig. 12.** "Expanded" uncertainty of normalized concentration, contours of different fuel injection mass flows.

Increasing the value of the normalized concentration an increment in the uncertainty occurs. This increment following constant fuel mass flow is at first linear and for higher values of the normalized concentration becomes exponential. The reason of this is that both the nominator and the denominator have an exponential trend but as shown before the uncertainty of [C] increases much more rapidly. For the same value of $[C]/C_{ref}$ and increasing the fuel mass flow an increment in uncertainty is presented as well. This particular increment is in fact higher for higher fuel mass flows since the iso-curves have a tendency of spreading. The "expanded" uncertainty presented again is a 95% normal distributed interval and shows the standard deviation of the mean value. For instance, a value of $[C]/C_{ref}=0.05$ for $m'_f=2.24$ yields an uncertainty of $\pm0.0018$. According to this, the mean relative error is 4.9%, 7.7%, 9.6% and 11.5% for the various values of $[C]/C_{ref}$. This clearly demonstrates that although $C_{ref}$ found to have $10^{-5}$ relative error the uncertainty from the FCP measurement ($e_r=20\%$) has affected the overall uncertainty. The final overall relative error has values greater of $10^{-5}$ but lower than 20%. Increasing the fraction of $C/C_{ref}$ the uncertainty increases and the error induced from the FCP has the leading role. Since the uncertainty of the calculated value has risen the design of the experiment should be changed and time-averaged quantities with small time between measurements for the concentration should be made in order to further decrease the induced uncertainty.

## 8 Conclusions

A probabilistic method for evaluating uncertainties in measurements and its application to pressure and fuel concentration measurements was presented.

As far as the pressure measurements are concerned the behavior of the uncertainty is the same for quantities expressed with the same form of mathematical expression. The absolute value of the uncertainty is strongly affected by the combination of different variables and how they are used in order to express the final result. The relative error from pressure measurements was in the margin of $10^{-5}\%$ to 0.1%.

On the other hand, the general method for quantifying an unknown uncertainty was presented for fuel concentration measurements. This method yields the uncertainty of a discrete variable. The induced relative error from the fuel concentration measurement found to be up to 20%. Also, the uncertainty induced from the calibration of the fuel concentration probe dissipates for higher values of concentration measurements; therefore the uncertainty of the result is affected more from the error of the analog-read of the microprocessor.

Combining the above measurements the uncertainty is affected from both measurands. The overall uncertainty of the combined result has accuracy (relative error) in the margin between the relative errors of the combined variables. Measuring higher values of concentration the uncertainty is affected from the big relative error of concentration measurements and the relative error of the combined measurements tends asymptotically to this particular error.

As a final conclusion, the Guide to the expression of Uncertainty in measurements presents a very robust and with high utility method of evaluating the uncertainty of measurements of all kinds. This method should be conducted during the design of the experiment in order to avoid unacceptable values in the uncertainty of the results. If unacceptable values of uncertainty do occur a normalization of the measurands or timeaveraged measurements should be considered. The uncertainties produced from this process are 95% or 99% normal distributed intervals in contrast with the 67% rectangular distributed interval the standard uncertainty quantification yields.

## References

1. A. Doukelis, K. Mathioudakis, *Turbomachinery Flow Measurements Using Long-Nose Probes*, GT2003-38488, Proceedings of ASME Turbo Expo 2003, Atlanta, Georgia, USA, June 16-19 (2003)

2. Gh. Al-Doori, R. D. Buttsworth, *Pitot Pressure Measurements in a supersonic stream jet*, J. Exp. Therm. Fluid Sci., **58**, p.p. 56-61, October (2014).

3. G. Zaragoza, R. Goodall, "Development of a device for the measurement of thermal and fluid flow properties of heat exchanger materials", *Journal of Measurement,* **56**, p.p. 37-49, October (2014).

4. Q. S. Li, S. Y. Hu, Y. M. Dai, Y. C. He, "Field measurements of extreme pressures on a flat roof of a low-rise building during typhoons", *Journal of Wind Engineering and Industrial Aerodynamics,* **111**, p.p. 14-29, December (2012)

5. A. Garinei, R. Marsili, *Measurement of pressure distribution on a membrane of a pump for biomedical applications through capacitive film sensors*, J. Meas., **55**, p.p. 110-116, September (2014).

6. Ch. S. McEnally, L. D. Pfefferle, *Species and Soot Concentration Measurements in a Methane/Air Nonpremixed Flame Doped With C4 Hydrocarbons*, J. Combust. Flame, **115**, Issues 1-2, p.p. 81-92, October (1998).

7.  X. Mercier, E. Therssen, J. F. Pauwels, P. Desgroux, *Quantitative features and sensitivity of cavity ring-down measurements of species concentrations in flames*, J. Combust. Flame, **124**, Issue 4, p.p. 656-667, March (2001).

8.  JCGM 100: (2008), GUM 1995 with minor correnctions, *Evaluation of measurement data-Guide to the Expression of Uncertainty in Measurements*, www.bipm.org

9.  T. Behr, A. I. Kalfas, R. S. Abhari, *A probabilistic uncertainty evaluation method for turbomachinery probe measurements*, The XVIII Symposium on Measuring Techniques in Turbomachinery Transonic and Supersonic Flow in Cascades and Turbomachines, 21-22 September, Thessaloniki, Greece

10. G. Stefopoulos, S. Rigas, P. Tsirikoglou, A. I. Kalfas, *Aerodynamic mixing performance investigation and validation of novel fuel air premixing devices*, Asian Congress on Gas Turbines 2014, 18-20 August, Seoul, Korea (2014)

11. K. Weise, W. Wöger, *Messunsicherheit und Messdatenauswertung*, WILEY-VCH Verlag, ISBN 3-527-29610-7, (1999).

12. Karsten Kusterer, Anas Elyas, Dieter Bohn, Takao Sugimoto, Ryozo Tanaka, (2008), *Double-jet Film-cooling for Highly Efficient Film-cooling with Low Blowing Ratios*, GT2008-50073, Proceedings of ASME Turbo Expo 2008, June 9-13, Berlin, Germany

13. Suman Muppidi, (2006), *Direct Numerical Simulations and Modeling of Jets in Cross Flow*, Dissertation Thesis, University of Minnesota

## Appendix A

Two different quantities are measured, $P_o$ and $P_{st}$. And the result obtained is the difference:

$$\Delta P = P_o - P_{st} \tag{13}$$

For every measured quantity an error of $\pm 0.05\%$ is present. Furthermore, by subtracting random variables the deviation does not subtract. According to this and using Eq. (3) the deviation induced from each random variable can be calculated as shown below:

$$u_{P_o}(\Delta P) = \left| \frac{\partial \Delta P}{\partial P_o} \right| u(P_o) \tag{14}$$

$$u_{P_{st}}(\Delta P) = \left| \frac{\partial \Delta P}{\partial P_{st}} \right| u(P_{st}) \tag{15}$$

And since the deviation of the measuring quantities is the same ($u(P_o)=u(P_{st})=0.05\%$) Eq. (14)&(15) yields:

$$u_{P_o}(\Delta P) = u_{P_{st}}(\Delta P) = 0.05\% \tag{16}$$

Finally, using the GEP (Eq. (4)) the overall uncertainty of $\Delta P$ can be calculated as follows:

$$u(\Delta P) = \sqrt{\left( u_{P_o}(\Delta P) \right)^2 + \left( u_{P_{st}}(\Delta P) \right)^2} \Rightarrow$$
$$u(\Delta P) = \sqrt{2} * u_{P_o}(\Delta P) = 0.0707\% \tag{17}$$